EARTH SURFACE PROCESSES AND LANDFORMS
Earth Surf. Process. Landforms **39**, 844–852 (2014)

Published online 3 March 2014 in Wiley Online Library
(wileyonlinelibrary.com) DOI: 10.1002/esp.3540

Letters to ESEX

Estimating fluvial wood discharge using time-lapse photography with varying sampling intervals

Natalie Kramer* and Ellen Wohl
Department of Geosciences, Colorado State University, Fort Collins, CO 80523, USA

Received 20 July 2013; Revised 25 December 2013; Accepted 27 January 2014

*Correspondence to: Natalie Kramer Anderson, Department of Geosciences, Colorado State University, Fort Collins, CO 80523, USA. E-mail: n.kramer.anderson@gmail.com

ESPL
Earth Surface Processes and Landforms

ABSTRACT: Monitoring large wood (LW: width >10 cm, length >1 m) in transport within rivers is a necessary next step in the development and refinement of wood budgets and is essential to a better understanding of basin-wide controls and patterns of LW flux and loads. Monitoring LW transport with coarse interval (≥ 1 min) time-lapse photography enables the deployment of monitoring cameras at large spatial and long temporal scales. Although less precise than continuous sampling with video, it allows investigators to answer broad questions about basin connectivity, compare drainages and years,and identify transport relationships and thresholds. This paper describes methods to: (i) construct fluvial wood flux curves; (ii) analyze the effects of sample interval lengths on transport estimates; and (iii) estimate total wood loads within a specified time period using coarse-interval time-lapse photography. Applying these methods to the Slave River, a large-volume (10^3 m^3 s^{-1}), low-gradient (10^{-2} m km^{-1}) river in the subarctic (60° N), yielded the following results. A threshold relationship for wood mobility was located around 4500 m^3 s^{-1}. More wood is transported on the rising limb of the hydrograph because wood flux declines rapidly on the falling limb. Five- and ten-minute sampling intervals provided unbiased equal variance estimates of 1 min sampling, whereas 15 min intervals were biased towards underestimation by 5–6%, possibly due to periodicity in wood flux. Total LW loads estimated from the 1 min dataset and adjusted for a 15% misdetection rate from 13 July to 13 August are: 1600 ± 200 # pieces, 600 ± 200 m^3 and of the order of 1.3×10^5 kg carbon. The total wood load for the entire summer season is probably at least double this estimate because only the second half of the summer was monitored and a large early summer peak freshet was missed. Copyright © 2014 John Wiley & Sons, Ltd.

KEYWORDS: wood; time-lapse; subarctic; sampling; rivers

Introduction

In-stream large wood plays an important and necessary role in the geo-eco-socio functioning of river corridors, coastlines and depositional basins. The presence of wood within channels is increasingly recognized as a contributing factor to large-scale change in fluvial forms and processes (Corenblit *et al.*, 2011; Collins *et al.*, 2012; Polvi and Wohl, 2013). In-channel wood facilitates complex channel flow, enhances hyporheic flow and creates more pool and backwater areas; thus its presence enhances the biogeochemical cycling of carbon by increasing residence times of particulate organic matter and dissolved organic carbon (Battin *et al.*, 2008; Skalak and Pizzuto, 2010; Wohl *et al.*, 2012). Export of wood to the oceans and storage of wood along riparian corridors, lake shores and basins are important for food webs and biodiversity (Gonor *et al.*, 1988; Everett and Ruiz, 1993; Naiman *et al.*, 2002; Gurnell *et al.*, 2005). Artificial introduction of wood for stream rehabilitation projects is a common management strategy (Beechie *et al.*, 2010). Large wood accumulations deposited during floods are considered when designing in-stream structures such as dams, weirs and bridges (Ruiz Villanueva *et al.*, 2013). Coastlines are stabilized from erosion by the presence of wood (Heathfield and Walker, 2011). And lastly, human communities often depend on driftwood as a fuel to heat their homes (Jones *et al.*, 2013).

Although many studies quantify, either in the field or via remote sensing, the potential stock of wood available for transport along streams and rivers (Abbe and Montgomery, 2003; Moulin *et al.*, 2011; West *et al.*, 2011), little effort has been employed in monitoring and quantifying wood in transport as it happens. The buoyancy of wood makes the use of imagery ideal for monitoring wood transport. Just as sediment gauges are integral for developing basin-wide sediment budgets, wood gauges, in the form of cameras, could be used alongside stream gauges to generate wood transport data to inform basin-wide wood budgets. At the most basic level, a wood budget is a change in wood storage along a reach equal to the inputs (from the hillside, bank and upstream) minus the outputs (export downstream or to long-term permanent storage on the floodplain). Previous attempts at generating wood budgets have focused on estimating recruitment volumes and changes in storage and then back-calculating wood export (Benda and Sias, 2003). However, this approach may be underestimating actual wood export by as much as a factor of ten (MacVicar

and Piégay, 2012). Recently, Schenk *et al*. (2013) tracked individual logs in transport using radio telemetry and combined those results with data from aerial photographs and on-site wood surveys to develop the first basin-wide wood budget on the low-gradient Roanoke River in North Carolina.

A first attempt at creating a wood transport curve used video monitoring of floods on the Ain River in France in 2011 (MacVicar and Piégay, 2012). The study focused on high temporal-resolution (continuous recording at 5 fps) video data over hydrograph peaks and then analyzed subsamples via an automated MatLab program. Three major conclusions were: wood transport begins at a threshold value of two-thirds bankfull discharge; wood discharge increases linearly with water discharge up to the bankfull discharge, after which it becomes much more variable as the flood plain is inundated; and wood transport rates are four times higher on the rising limb than the falling limb (MacVicar and Piégay, 2012).

While video monitoring provides high temporal-resolution data useful for computing rates of transport and fine-scale relationships between wood and water discharges, time-lapse photography allows a researcher to sample at broad spatial and long temporal scales. Investigations at broad scales that answer questions about basin connectivity are integral as river scientists attempt to quantify system resilience and make recommendations for managers in an increasingly uncertain future. Sampling at long intervals (minutes) is also extremely advantageous for studies with small budgets which seek to install networks of cameras to be left up for months. This is especially true for remote areas where access, travel costs or project costs limit the practicality of video monitoring.

This study is part of a larger study investigating wood transport in large rivers and export of LW to the Arctic from the Mackenzie Basin, Canada. Part of the larger study involves basin-wide questions of wood connectivity, differences in transport thresholds between tributaries and relationships between wood export and ice jam processes. Prior to installing a network of eight remote cameras to be left up for months in a basin which drains 20% of Canada, this study was conducted to develop procedures to: estimate LW fluxes and total loads during high flows with non-continuous coarse data; and identify unbiased, equal-variance coarse sampling intervals with the overall goal of selecting the coarsest sampling interval possible in order to minimize post-processing time, on-site power usage and memory storage. Using non-continuous data from timelapse photography, this paper describes methods to: (i) construct fluvial wood flux curves as probabilities, (ii) analyze the effects of sampling interval lengths on flux estimates, and (iii) estimate total wood loads within a specified time period.

The Slave River Study Site

The Slave River begins at the confluence of the Peace River with the Athabasca Delta and flows north for 430 km, providing 74% of the inflow to the Great Slave Lake (Gibson *et al*., 2006), one of the world's deepest lakes and the origin of the Mackenzie River. The Slave River drains approximately 6×10^5 km^2, with much of its water originating from the melting of mountain glaciers and snowpack in the Canadian Rockies in southern Alberta. The Slave River freezes every winter and there are generally two hydrograph peaks: the first corresponds to ice break-up and the second is a freshet peak related to runoff from snowmelt. However, not all years have a large ice break-up flooding event because it is dependent on river flows and the formation and location of ice jams (Beltaos *et al*., 2006). In some years, large releases from the W. A. C. Bennet Dam (built 1963–1968, filled by 1971) on the Peace River and/or large summer rain events can cause late-summer secondary peaks.

The Slave River flows through boreal forest, and recruitable trees along the river corridor are predominantly fairly small (<30 cm diameter) aspens and white spruce. However, it is common to find driftwood tree boles of poplars and conifers 30–80cm in diameter (without bark) and 10–20 m in length (many snapped) in the vicinity of the field site (unpublished data). This suggests long travel distances (10^2-10^3 km) of in-stream wood recruited from the northern Alberta plains and mountainous forests of the southern Canadian Rockies where trees are larger. Although not addressed in this study, ice processes likely play a large role controlling annual flux of wood from the Slave and other northern rivers. Trees which fall into the river via bank failure or are stranded by high flows are routinely transported by ice jams and associated floods.

A camera was installed next to the 'Slave River at Fitzgerald' gauge 7NB001 operated by Water Survey Canada (1921–present). Based on a survey on 12 May 2011 by Water Survey Canada, the cross-sectional area is around 5000 m^3 with bottom depths of 8–12 m and a surface width of 300 m. The upstream gradient is 10^{-2} m km^{-1} and the gross drainage area is 6.06×10^5 km^2. Summer flows generally range from 2000 to 6000 m^3 s^{-1}, and the highest recorded flow was 11 200 m^3 s^{-1} on 5 May 1974 during an ice break-up event. The 1.5 year flood is 5700 m^3 s^{-1} based on 45 years of data from 1966 to 2011. Ice break-up occurs in May, freshet peaks occur in June and July, baseflows are reached by September and freeze-up occurs in November.

The 10 cm diameter and 1 m length cutoff for LW commonly used in instream wood studies (Naiman *et al*., 2002), and the 20 cm diameter and 3 m cutoff used by Schenk *et al*. (2013), are both reasonable approximate size thresholds for the Slave River based on analysis of size distributions of logs measured in downstream jams (Figure 1). For this site, the upper threshold was adjusted to 0.23 m diameter based on a natural break in the data (Figure 1). Following convention, all pieces greater 10 cm in diameter and 1 m in length are considered as LW, with

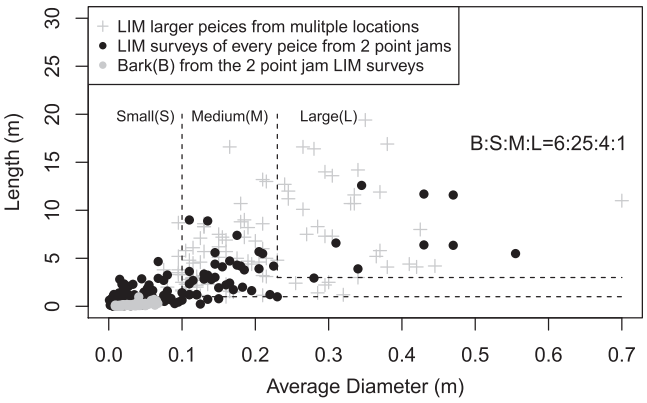

Figure 1. LW size thresholds from point jams. Wood pieces were measured along transects using the line intersect method (LIM) in jams within 20 km downstream of the camera location in 2012. Transects were laid along the entire length of the jam perpendicular to piece orientation. Any piece crossing the line was measured for its length and two end diameters. The *x*-axis in this plot is the average of the two end diameters. For two transects, lines were drawn with spray paint and any piece with paint on it, no matter how small, was counted. These two surveys are represented as filled circles, black denotes sticks or logs and grey denotes bark (B). The grey plus signs represent logs from transects from which only logs>10 cm in diameter(d) and >1 m in length(l) were measured. The dashed lines are drawn at two thresholds, dividing the log pieces into three categories: small (S) < d = 10 cm, l = 1 m ≤ medium (M) < d = 23 cm, l = 3 m ≤ large (L). Using these thresholds, the point jam piece size ratio was 6(B):25(S):4(M):1(L).

pieces smaller than this identified as small wood. An extension to this categorization is that LW pieces less than 23 cm and 3 m are considered medium LW, and pieces greater than 23 cm and 3 m are considered large LW. The point jam ratio of small:medium:large was 25:4:1. Using a simple formula for a cylinder (tree boles are usually stripped of branches and are fairly straight) and ignoring rootwads, the average LW piece volume was 0.35 m^3, $s^2 = 0.31$ for $n = 127$. Most of the variance in LW volumes comes from the variance of large LW, which had a mean volume of 1.01 m^3, $s^2 = 0.52$ for $n = 35$. In comparison, the mean volume for medium LW was 0.09 m^3, $s^2 = 0.01$ for $n = 92$. These are minimum estimates because they do not include rootwad volumes. Approximately one-third of the LW logs measured from point jams had rootwads. More work needs to be conducted to develop rootwad volume relationships with easily measured metrics.

Data Collection

In the summer of 2012, an Olympus X560WP camera connected to an intervalometer captured photos at 1 min intervals for 32 days from 13 July to 13 August. Not all days were monitored within the study period. The camera was not functioning on 18 July, 23–27 July or 1–8 August. The camera was placed on the outside of a bend constricted by a bedrock point and looked out across the river (59° 51′ 48″ N, 111° 35′ 28″ W, 120° azimuth).

For the majority of the channel and the majority of the flows, it took close to, or longer than, 1 min for a log to traverse the field of view. Therefore, the 1 min dataset is assumed to represent the true count of logs during the sampled periods. The thalweg transported most wood (90% based on an hour of on-site observation) closer than 100 m to the bank with downstream transport distances of 20–100 m in the field of view. The channel length captured by the camera for the far shore is around 400 m. The average velocity calculated by dividing discharge by cross-sectional area ranged from 40 to 60 m min^{-1} throughout the study period. Surface velocities measured by Water Survey Canada on 12 May 2011 during a discharge of 4700 $m^3 s^{-1}$ ranged from 12 to 150 m min^{-1}. The peak flow during the study period was 5000 $m^3 s^{-1}$, the average flow was 4000 $m^3 s^{-1}$ and the minimum flow was 3400 $m^3 s^{-1}$.

A total of 12 761 photos were manually analyzed for presence/absence and number of easily identifiable pieces of LW such as tree boles, rootwads and larger branches. If present, the number of pieces in each photo were tallied. If a log was circulating in the eddy near the shore or if it was at the top of one frame and the bottom of the next, it was not counted more than once. In total, 652 logs were counted and 7% of them had rootwads. This task was not automated because the human eye performs better than automated object identification schemes and the goal of the study was to analyze the effects of sampling at coarser intervals, not the detection of error rates for automated techniques.

In order to obtain an idea of error associated with miscounted logs in images, an hour was spent on-site viewing and recording logs in transport in 2013. When wood floated by the camera, the time, distance from shore (close: <60 m; or far: >60m) and approximate size (small, medium or large) were noted. Small pieces included sticks and branches estimated to be under the 10 cm in diameter and 1 m in length cutoff for LW. Medium and large pieces were tree boles or large branches.Large pieces were estimated to be greater than 23 cm in diameter and 3 m in length based on piece size distributions measured from downstream jams (Figure 1). During the hour, a total of 102 pieces were counted and the ratio of small:medium:large pieces was 20:3:1. This ratio is similar to the ratio of 25:4:1 obtained from jams; thus the average piece size on point jams is likely a good approximation of average piece size for logs in transport. Counted logs were then compared to wood identified on photos taken during the same time period at intervals of 30 s. Small pieces were generally not seen in the images. Twenty LW pieces (medium or large) were counted with a success rate of 85% (17/20). Thirteen of the 20 logs were correctly counted, while 4 of 17 logs were counted although they were not actually present. All of the logs that were missed were medium-sized logs marked as far from shore. There was 100% recognition of large logs at any distance and medium logs close to shore. From on-site field observations of floating wood, most logs were not waterlogged and floated high on the surface; thus error rates due to sunken logs are assumed to be negligible.

Wood Flux as a Probability

Statistical methods

Calculating wood flux as probability of occurrence (proportions of photos) is very advantageous because it does not depend on wood size or count, effectively eliminating large uncertainties with calculating these metrics. It also allows for easy comparison across drainages with different wood sizes and facilitates quick post-processing of photos. In order to calculate a wood flux as a probability, only presence/absence needs to be noted. An additional level would be to include several quick categorizations (e.g. absent, single, sparse, clumped, congested or carpet) and the probabilities of each. During this study, there was only sparse wood transport, so categories were not utilized.

Unlike monitoring water discharge, it is impossible to ever obtain complete absolute values of wood flux because there will always be data gaps at night when it is too dark to capture good imagery. Additionally, there are often data gaps when equipment isnot working or not installed. Stratification of proportion estimates (by time, by discharge or by any other scheme) allows comparison between strata categories with unequal number of photos and extrapolation of data into unsampled time periods. Precision will always be increased when stratification is used if variance within strata is minimized while variance between strata is maximized (Scheaffer *et al.*, 2012).

For the Slave River case study, both stratification by day and stratification by discharge were utilized. Daily proportions are the probabilities, for any given moment, in any given day, of seeing wood in transport. Discharge proportions are the probabilities of seeing wood in transport for specified ranges of flows. Stratification by day was used to obtain insights into how LW flux relates to water discharge. Stratification by discharge was used to estimate total LW loads despite data gaps of more than 1 day.

Proportions, $\hat{p}$, and variances, $\hat{V}(\hat{p})$, were estimated based on systematic sampling of a finite population (Scheaffer *et al.*, 2012, p. 228):

$$\hat{p} = \sum_{i=1}^{n} \frac{y_i}{n}, \quad \hat{V}(\hat{p}) = \frac{\hat{p}\hat{q}}{n-1}\text{fpc} \tag{1}$$

where $\sum_{i=1}^{n} y_i$ is the total number of photos with logs present, n is the total number of photos sampled (sample size), $\hat{q}$ is $1 - \hat{p}$, fpc is the finite population correction factor $\frac{(N-n)}{N}$ and N is the finite population, the total minimum number of frames needed to uniquely capture the entire wood load within a period of interest. If the entire period of interest was sampled at intervals equal to the amount of time for a log to travel across the frame, the proportion can be computed exactly ($\hat{V}(\hat{p}) = 0$). For $n \ll N$ the fpc approaches 1 and $\hat{V}(\hat{p})$ approaches the equation for an

infinite population. For this study, 1 min intervals were used to estimate N since this was the approximate amount of time that it took a log to traverse the field of view during sampling periods (see 'Data Collection', above).

If stratification was desired, $\hat{p}$ and $\hat{V}(\hat{p})$ were estimated using double sampling for stratification:

$$\hat{p}_{st} = \sum_{i=1}^{L} \hat{w}_i \hat{p}_i, \qquad (2)$$
$$\hat{V}(\hat{p}_{st}) = \frac{\text{fpc}}{n-1} \sum_{i=1}^{L} \hat{w}_i \hat{p}_i q_i + \frac{1}{n^2} \sum_{i=1}^{L} (1 - \hat{w}_i) \hat{p}_i q_i$$

where L is the number of strata and $\hat{w}_i = N_i/N$, the weight for each stratum. Weights were calculated post-sampling as the proportion of the population (total # of intervals) in each stratum. p_i was calculated using Equation (1) for each stratum and 95% confidence intervals were constructed using a bound of $2\sqrt{\hat{V}(\hat{p}_{st})}$. $\hat{V}(\hat{p})$ is the sum of two terms. The first term is the variance of the sampling, while the second term penalizes for choosing strata after the fact (the number of samples within each stratum was not known prior to sampling). In most cases, the second term rapidly approaches zero as n increases and can be considered negligible (this study included).

Slave river results

Within this 32-day study (13 July to 13 August), LW flux ($\hat{p}$) ranged from zero to just under 20% and peak values corresponded well with a freshet peak in mid July (Figure 2, top). The estimated probability from sampled images over the entire study period was near 4% (Table I). Precision on this estimate was increased by 6% and 9% if stratification by day and by discharge were utilized (Table I). Strata by discharge included two groups: $Q < 4500$ m^3 s^{-1} and $Q > 4500$ m^3 s^{-1} based a transport threshold identified by comparing daily water discharges to daily wood fluxes (Figure 2, bottom).

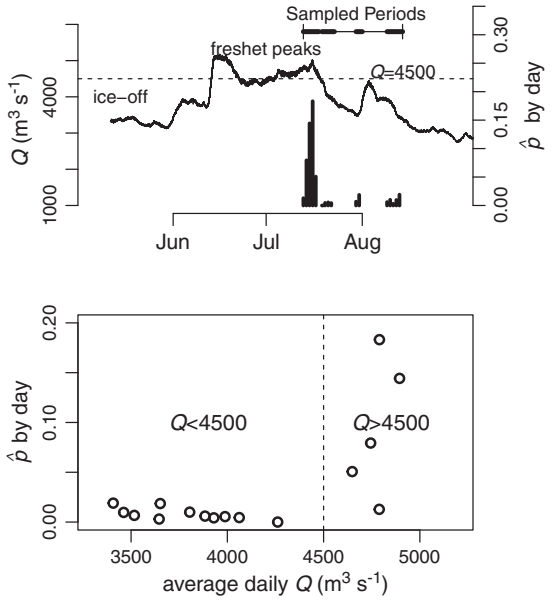

Figure 2. Wood flux and transport thresholds, Summer 2012. Top: comparison of wood flux as daily probabilities (bars) to water discharge (Q) over the study period. The horizontal line segment at the top of the graph shows the time period (13 July to 13 August) over which the total wood loads were estimated. Sampled periods are depicted as thicker bars. Unfortunately, due to a camera malfunction, data were not gathered over the apex of the humped peak in late August. For this year, ice-off occurred on 8 May without ice jam flooding. However there were two prominent freshet peaks. Camera installation occurred after the first peak, but captured the second. Bottom: daily probabilities of seeing wood in transport versus discharge. A transport threshold of $Q = 4500$ m^3 s^{-1} is identified and shown in both graphs.

Analysis of Sampling Intervals

Statistical methods

In order to examine the effects of sampling interval on LW flux and load estimates, data were split into sub-datasets at fixed 5, 10 and 15 min intervals. Because the intervals are fixed, there were five 5 min datasets, ten 10 min datasets and fifteen 15 min datasets. Henceforth, each dataset within a sampling period will be referred to as a trial. Variances were calculated with the population total N equal to the 1 min dataset rather than total number of 1 min photos possible over the entire study period (see Equation (1) and Table I). This was done to use the collected 1 min data as the known true population, p, when comparing the effects of sampling at coarser intervals. Errors of estimation were calculated daily and for the whole time period as $\hat{p} - p$, where $\hat{p}$ is the estimate of p obtained from the 5, 10 and 15 min trials. When the error of estimation is negative, $\hat{p}$ underestimates and visa versa.

To compare variances and bias between sampling intervals, it is necessary to make the sample size of each trial over all sampling intervals equal via bootstrapping. A simple random sample of size $n = 100$ for each 5, 10 and 15 minute trial was repeatedly sampled 10 000 times. The mean $\hat{p}$ and $\hat{V}(\hat{p})$ were calculated for each trial, and the average of all the trials within each time interval $\bar{\hat{p}}$ was compared to the population value p from the 1 min data.

Slave river results

Non-stratified proportions of photos with wood present were calculated for each trial using Equation (1). While the 5 and 10 min intervals provided unbiased estimates of the 1 minute proportion ($+10^{-4}$%), the 15 min dataset was biased towards underestimating the actual value by about 5% (Figure 3 and Table II).

All daily estimates of proportions for 5, 10 and 15 min trials in relation to the 1 min data are shown in Figure 4 for the freshet peak in mid July. Proportions have much more variability on the rising limb than the falling limb for all trials. Most trials capture the peak in the 1 min data, but the 15 min trials

Table I. Comparison of stratification versus non-stratification on $\hat{p}$ and its precision for the complete 1 min dataset from 13 July to 13 August

	$\hat{p}$	$\hat{V}(\hat{p})$	Bound	%Δ Precision
No stratification	$4.14e^{-2}$	$2.23e^{-6}$	$3.00e^{-3}$	—
Stratified by Q	$4.14e^{-2}$	$2.11e^{-6}$	$2.91e^{-3}$	+6.25
stratified by day	$4.14e^{-2}$	$2.06e^{-6}$	$2.87e^{-3}$	+9.10

The finite population total was estimated to be the number of possible frames taken at 1 min intervals within these 32 days ($N = 46080$). Q was stratified based on a 4500 m^3 s^{-1} threshold for transport (Figure 2). Refer to Equation (1)for the calculations of $\hat{p}$, $\hat{V}(\hat{p})$, and Bound. %Δ Precision was calculated as change in $1/\hat{V}(\hat{p})$ from no stratification.

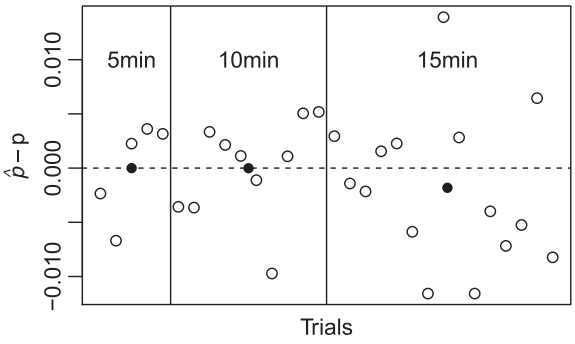

Figure 3. Error of estimations for all trials. Open circles represent errors from the 1 min data calculated for each trial, closed circles are the average error of all trials for each interval. Circles plotted on the dashed line show very little to no difference relative to the 1 min dataset.

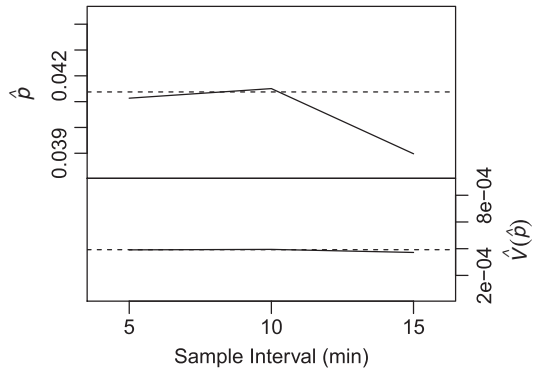

Figure 5. Comparison of proportions and variance across sample intervals using bootstrap sampling to achieve equal n. Each trial was sampled for $n = 100$, 10000 times and averaged. All trials were then averaged to obtain an estimate for each sample interval. Dashed lines represent values from the 1 min dataset.

Table II. Mean errors over all trials for each interval

	5 min	10 min	15 min
$\hat{p} - p$	$2.34E^{-7}$	$3.58E^{-7}$	$-2.20E^{-3}$
% difference	$5.67E^{-4}$	$8.66E^{-4}$	−5.30

$\hat{p}$ is the estimated proportion of photos with wood over the entire sampling period for each interval and p was estimated from the 1 min data to be $4.14E^{-2}$.

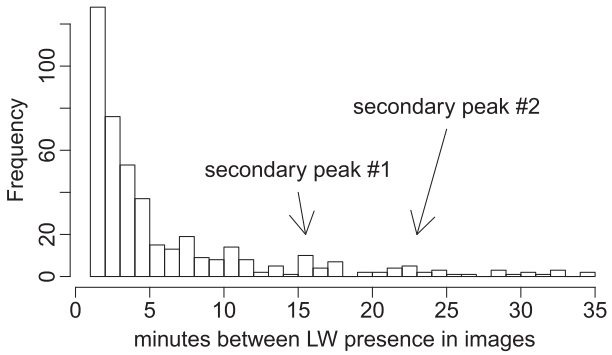

Figure 6. Frequencies of lag times between LW presence in images. Time between presence decays fairly rapidly and evenly from 1 min to about 14 min. This is expected since most wood is transported within 4 consecutive days of the 32-day study period (Figure 2). After the curve decays to near zero at 14 min, there appears to be a slight secondary jump in the number of instances corresponding to a 15–18 min lag between wood transport. A second, yet more subtle hump occurs between 20 and 25 min.

appear to consistently underestimate peak values and do a poor job characterizing the steep falling limb. The daily errors of estimations confirm this pattern (Figure 4). While the 5 and 10 min datasets appear to be evenly split between under- and overestimating the true proportion, the 15 min data consistently underestimate. In addition, the errors are two to three orders of magnitude larger for the 15 min data compared to the 5 or 10 min data, most notably near peak wood transport.

Although the 15 min trials are biased towards underestimation, bootstrap sampling clearly demonstrates that the variance is stable across all sample intervals (Figure 5). Although not shown, the data were unbiased up to 14 min. This sudden bias at 15 min suggests that there may be some periodicity in the data. This idea is somewhat supported by a slight jump in the number of instances corresponding to a 15–18 min lag between wood presence in images (Figure 6).

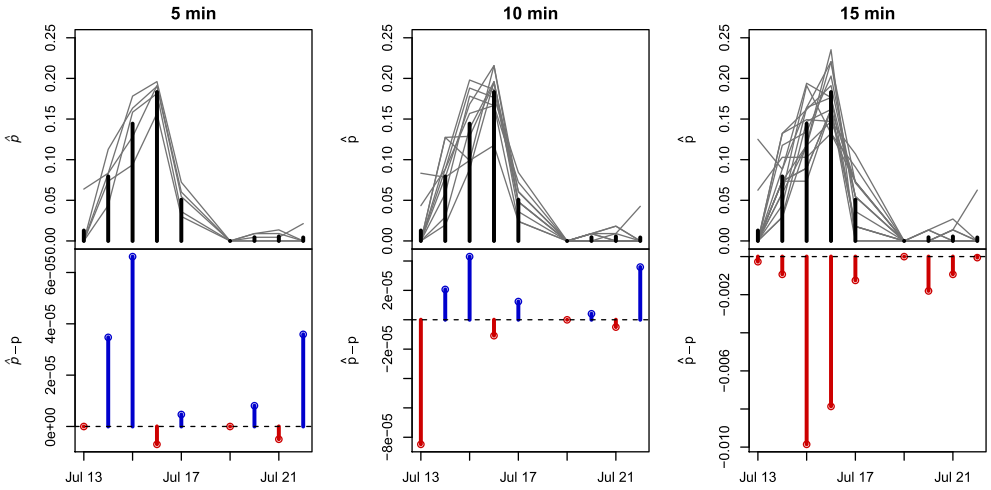

Figure 4. Time series of each trial over the freshet peak with daily errors. Solid bars show p from the 1 min data and grey lines are the $\hat{p}$ estimates from each trial. The lower half of each graph shows daily errors. The dashed line is drawn at zero error. Solid error bars were calculated by averaging the errors from each trial and then subtracting from the 1 min dataset. This figure is available in colour online at wileyonlinelibrary.com/journal/espl

Calculating Total Wood Loads

Statistical methods

The following equations calculate, in steps, the estimates for total wood loads (count and volume) within a period of interest. By calculating in steps, imprecision for each component can be clearly compared to other components. Sampling strategies can be employed to focus efforts on reducing variability in the most efficient manner by addressing components with the most imprecision.

For each stratum of interest, estimate:

(1) Total number of frames that logs are present:

$$\hat{T}_f = N\hat{p}, \qquad \hat{V}\left(\hat{T}_f\right) = N^2\hat{V}(\hat{p}) \tag{3}$$

where N is the number of frames within a set time interval it takes a log to traverse the field of view and $\hat{p}$ and $\hat{V}(\hat{p})$ are computed using Equation (1). N is essentially the minimum number of frames (moments in time) needed to capture the entire LW population within a stratum in a study period. For the Slave River, N was estimated to be the number of 1 min intervals within each stratum for the 32-day study period (see 'Data Collection', above, for justification). However, N could be adjusted to account for changing velocities. This may be useful for rivers with rapidly varying flows.

(2) Total count of logs:

$$\hat{T}_c = \hat{T}_f\overline{c}, \qquad \hat{V}\left(\hat{T}_c\right) = \hat{T}_f^2\hat{V}(\overline{c}) + \overline{c}^2\hat{V}\left(\hat{T}_f\right) \tag{4}$$

where $\overline{c}$ is the average number of logs in a photo when logs are present, s is the sample standard deviation and $\hat{V}(\overline{c}) = s^2/nf\mathrm{pc}$. For this study, the entire sample was used, but $\overline{c}$ could also be computed using a subsample, which could greatly increase processing efficiency. Within any population smaller subsamples will be less precise than larger ones. If a population has high variance, more samples will need to be included to achieve the same precision as a population with low variance.

(3) Total volume of logs:

$$\hat{T}_v = \hat{T}_c\overline{v}, \qquad \hat{V}\left(\hat{T}_v\right) = \hat{T}_c^2\hat{V}(\overline{v}) + \overline{v}^2\hat{V}(\overline{c}) \tag{5}$$

where $\overline{v}$ is the average volume per log and $\hat{V}(\overline{v}) = s^2/n$, the sample variance. The average volume per log could be calculated from a sample of the captured images, estimated or measured from jams downstream. If $\overline{v}$ is measured directly from the sampled images, a finite population correction factor should by applied to the variance, as in Equation (1).

To compute total LW loads over an entire period of interest, sum over all strata and compute a bound. For the equation below, T_i denotes any of the above totals from a single stratum:

$$\hat{T} = \sum_{i=1}^{L} T_i, \qquad \hat{V}\left(\hat{T}\right) = \sum_{i=1}^{L} \hat{V}(T_i), \qquad \mathrm{Bnd}_{95\%\mathrm{CI}} = 2\sqrt{\hat{V}\left(\hat{T}\right)} \tag{6}$$

A carbon load can be calculated by multiplying the total volume estimate by an average density and then multiplying by the of fraction carbon.

Slave river results

Three main assumptions were made during the calculation of wood loads for the Slave River: (i) the sampled periods are good representations of the unsampled flows; (ii) a log traverses the field of view at about 1 min intervals for the duration of the study; and (iii) logs measured in jams are representative of the size distributions of large logs captured on the images. The first assumption is reasonable because most of the unsampled flows occurred beneath the 4500 $m^3 s^{-1}$ transport threshold and wood transport under this threshold had low variance (Figure 2, bottom). Based on on-site observation, the unsampled peak in late August transported wood at similar rates to sampled periods under 4500 $m^3 s^{-1}$. Wood available for transport is likely stored along banks higher than flows < 4500 $m^3 s^{-1}$ can mobilize.

The second assumption, that a log traverses the field of view at about 1 min intervals for the duration of the study, is reasonable based on image analysis and an analysis of velocity ranges (see 'Data Collection', above). Although more rigorous estimation of the total number of frames needed to uniquely characterize the wood load is possible by accounting for changes in velocity, using an approximation based on 1 min intervals was deemed acceptable to obtain first-order estimates of wood flux and loads. Uncertainty due to this factor was not included in the estimate of total wood loads. An improvement to the techniques presented here would be to rigorously estimate the minimum number of theoretical frames needed to capture the entire population of drift logs by incorporating changes of velocity. Due to variability in velocities in wood transport paths, uncertainty in river cross-sections and variability in channel length in the field of view, this is actually quite challenging to do. Futurework comparing time-lapse at short time intervals to continuous video monitoring may help to constrain these estimates.

The third assumption, that logs measured in jams are representative of logs captured in images, is also reasonable. The size ratio of small:medium:large logs from jams (25:4:1), is similar to the ratio derived from on-site monitoring of wood in transport (20:3:1) (see 'Data Collection', above). Jams were measured the first season after they were deposited by large wood flux in 2011 and were positioned above the high-water level for 2012. Thus little to no winnowing of smaller pieces had occurred prior to measurement. Jams were also not reorganized by ice because no ice jamming events were recorded by the upstream gauge in 2012. Measuring logs directly from images has large uncertainties given distortion from oblique viewing, submergence of parts of logs and uncertainties of widths (MacVicar and Piegay, 2012). Estimating volumes and sizes of wood in transport based on measurments made from large logs in temporary storage can be a valuable proxy to measuring logs directly from images.

Wood loads from 13 July to 13 August were calculated based on proportion estimates stratified by discharge (Table III). 28% of the study period was sampled. During peak transport ($Q > 4500$ $m^3 s^{-1}$), 53% was sampled. Although stratifying by day increased precision more than stratifying by discharge, it was not used to estimate total LW loads because not all days were monitored (Figure 2). Ice break-up and the first major freshet peak were not monitored; thus the wood loads presented are not the total estimate for the year but just for the second half of the summer. Because the majority of wood transport likely occurred during the first freshet peak in mid June (Figure 2), the total yearly wood load for 2012 is probably more than double the values summarized below.

Table III. LW load estimates for the study period (13 July to 13 August) calculated from the 1 min data using Equations (1–6). Estimates include a 95% confidence interval of $\pm 2\sqrt{\text{variance}}$

	n	N	n/N	$\hat{p}$
$Q \leq 4500$	8643	38322	0.23	$0.08E^{-1} \pm 0.02$
$Q > 4500$	4118	7758	0.53	$1.11E^{-1} \pm 0.09$
$Q = All$	12761	46080	0.28	$0.41E^{-1} \pm 0.03$
	$\hat{T}_f$	$\overline{c}$	$\hat{T}_c$	$\hat{T}_v$
$Q \leq 4500$	306 ± 66	1.01 ± 0.03	310 ± 68	109 ± 39
$Q > 4500$	864 ± 73	1.27 ± 0.04	1096 ± 97	384 ± 114
$Q = All$	1170 ± 98	1.24 ± 0.04	1406 ± 119	492 ± 120

n is the total number of frames sampled.
N is the total number frames needed to uniquely characterize the wood load.
n/N is the proportion of the population sampled.
$\hat{p}$ is the estimated proportion of time LW was present (Equation (1) or (2)).
$\hat{T}_f$ is the total estimated population of frames with LW present (Equations (3) and (6)).
$\overline{c}$ is the average number of LW pieces per frame.
$\hat{T}_c$ is the total estimated count of LW (Equations (4) and (6)).
$\hat{T}_v$ is the total estimated volume of LW in m^3 (Equations (5) and (6)). An estimated average piece volume of $\overline{v} = 0.35$ m^3, $V(\overline{v}) = 2.4E^{-3}$ was used (see 'Data Collection' and Figure 1).

The total LW loads, estimated from the 1 min data, are 1406 ± 119 # pieces ($\hat{T}_c$), 492 ± 120 m^3 ($\hat{T}_v$) and of the order of 1.1×10^5 kg carbon. The misdetection analysis presented in the 'Data Collection' section above suggests a detection rate of 85%, meaning that these estimates are underestimating actual load by about 15%. The wood loads, adjusted to take this misdetection into account and rounded so that more precision than present is not implied, are 1600 ± 200 # pieces ($\hat{T}_c$), 600 ± 200 m^3 ($\hat{T}_v$) and of the order of $1.3E^5$ kg carbon. The bounds for $\hat{T}_c$ and $\hat{T}_v$ were both rounded up instead of down in order to include any additional uncertainties that are unaccounted for. For this study, mass of carbon was estimated assuming an average density of 450 kg m^{-3} (the main tree species are poplar, aspen, white spruce, birch and larch) and a 0.50 fraction of carbon (Lamlom and Savidge, 2003). The carbon estimate does not include a bound because uncertainties associated with the density or fraction of carbon are unknown.

The total count of logs, $\hat{T}_c$, from the 1 min data is more precise than the total volume, $\hat{T}_v$ (Table IV). After comparing variance contributions in Equations (3–6), it was determined that the imprecision in the $\hat{T}_v$ estimate is largely due to imprecision in average volume per log ($\overline{v}$). Most of the variance in $\hat{T}_v$ originates from variance in $\overline{v}$ (86%) rather than the variance in $\hat{T}_c$. The variance in $\hat{T}_c$ mostly originates from variance in $\hat{p}$ (92%), rather than variance in the average number of pieces per frame ($\overline{c}$).

Precision and accuracy of LW load estimates are compared across sampling intervals in Table IV and Figure 7. While the 5 and 10 min data are unbiased compared to the 1 min data, the 15 min data underestimates by about 6.5%. When bounds are compared to the 1 min data, the 5, 10 and 15 min data are 2.4, 3.4 and 4 times less precise for the total count and are 1.3, 1.5 and 1.7 less precise for the total volume, respectively. By comparing percentage error between count and volume, the 1, 5, 10 and 15 min count estimates are 2.7, 1.5, 1.3 and 1.2 times as precise as volume, respectively. Figure 7 shows the 95% confidence intervals about the total count estimate for each trial. All trials for the 5and 10 min data plot within the confidence interval of the 1 min data, while 13% of the 15 min trials plot outside the 1 min confidence band (dashed lines).

Based on these results, a network of eight cameras were installed in 2013 on major tributaries of the Mackenzie River, Canada, and set to take pictures every 10 min. The Olympus X560WP camera connected to an intervalometer was not used. Although the pictures were excellent, it was found that this set-up used too much power to be practical without regular access. Instead, A Brinno TLC200 time-lapse camera ($150) with waterproof housing was connected to a 6 V Energizer battery. Although this set-up captured lower-resolution photographs, wood could still be reliably seen on images. Photographs captured at 10 min intervals from 17 March to 9 July in 2013 used 0.15 V and only 1 GB of memory. Images taken with this camera are stored as a movie file with a user-defined frame rate. During periods of wood transport, individual frames can be exported from the movie for detailed analysis.

Discussion

The methods presented are a good way to gather broad spatial and long temporal wood transport data. Although imprecise, these methods can be very useful to examine trends along a

Table IV. Comparison of LW load estimates between sampling intervals

	1 min	5 min	10 min	15 min
Total count				
$\hat{T}_c$ (m^3)	1406 ± 119	1406 ± 287	1406 ± 409	1314 ± 482
% error	9	20	29	37
Total volume				
$\hat{T}_v$ (m^3)	492 ± 120	492 ± 151	492 ± 183	460 ± 200
% error	24	31	37	44

Estimates for each sample interval were computed by averaging the results for the trials within that sampling interval (see Figure 7). Load estimates were obtained stratifying by Q, as shown in Table III. % error = (bound/estimate) $\times 100$.

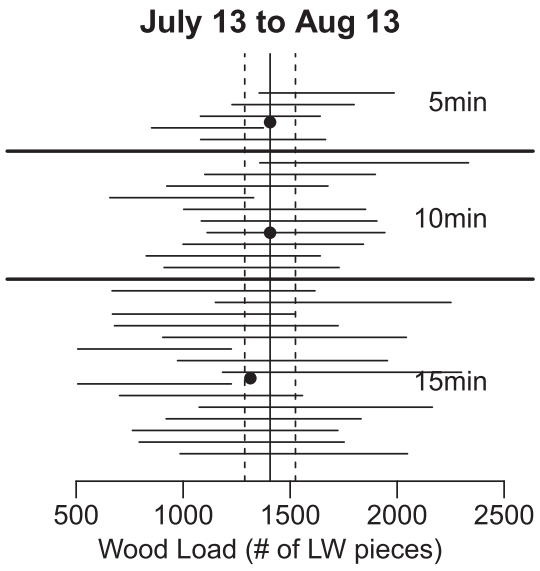

Figure 7. Total LW count estimates showing variability between trials. Horizontal lines are the 95% confidence intervals in total wood load for each trial. The solid vertical line and two dashed lines mark the estimate from the 1min data and its 95% confidence interval. Filled points mark the average estimate over all trials for each sampling interval summarized in Table IV.

drainage network and trends through time, to help constrain wood and carbon budgets, and to show general relationships between water flux and wood flux. Sampling at coarse intervals extends the amount of time cameras can be left without maintenance by saving memory space and battery usage. When project budgets are too tight to install fully equipped monitoring stations with solar panels and automatic downloads, the use of coarse-resolution time-lapse photography sampling provides a cost-effective way to monitor and estimate wood loads. Coarse interval sampling also greatly reduces the amount of post-processing time by reducing the number of photos to analyze.

For the Slave River, time-lapse sampling at less than 15 min provides imprecise, unbiased, equal-variance estimates of 1 min data (Tables II and IV). Periodicity in wood flux will bias results for regular interval sampling if sampling interval is close to the wavelength of the periodic flux. There may a slight periodicity in flux for the this site of around 15–18 minutes (Figure 6), which may be the cause of the underestimation bias in the 15 min dataset. Future work should focus on analyzing wood flux periodicity and relating it to drivers such as water and/or recruitment fluxes.

Appropriate sampling intervals to achieve unbiased estimates may be related to hydrograph and wood recruitment regimes. For rivers similar to the Slave River, characterized by less variable hydrographs (rise and fall of a peak flow takes many days) and wood recruitment driven by hydrology rather than upslope processes, sampling at 5 or 10 min intervals should be adequate to achieve unbiased estimates of wood load. For drainages with short event durations, it is likely that sampling every 5 or 10 min may no longer provide unbiased estimates due to undersampling compared to rates of change.

Although caution should be used when applying results from this study to drainages with flashier hydrographs and/or more episodic wood recruitment dominated by landslides, the statistical and estimation methods discussed here can be used to determine appropriate sampling intervals. Additional analyses from many basins need to be conducted to determine if there exists universal thresholds or predictable relationships for sampling intervals which yield unbiased, equal-variance estimates of finer sampling intervals and to illuminate processes and patterns of wood flux across regions. Analysis of wood flux, sampling interval and rates of change in water discharge between locations, events and years would be an interesting future endeavor.

A valuable outcome of monitoring wood fluxes using time-lapse cameras is the rapid identification of transport thresholds. MacVicar and Piégay (2012) identified a threshold for transport near 2/3 bankfull. The 1.5-year flood (a proxy for bankfull) for the Slave River is 5700 $m^3 s^{-1}$ and two-thirds of that is 3800 $m^3 s^{-1}$. A 3800 $m^3 s^{-1}$ LW transport threshold seems high for the Slave River (Figure 2, bottom), but is close because there was less than 1% probability of transport for flows less than 4500 $m^3 s^{-1}$ (Table III). The 4500 $m^3 s^{-1}$ threshold identified in this study is similar to a 4000 $m^3 s^{-1}$ threshold for ice jam flooding on the Slave River's primary tributary, the Peace River (Beltaos *et al.*, 2006).

Estimates of total LW loads are useful for refining and computing LW or carbon budgets. After a 15% upward adjustment for misdetection errors, the total loads for the Slave River between 13 July and 13 August were estimated to be 1600 ± 200# pieces, 600 ± 200 m^3 and of the order of 1.3×10^5 kg carbon. These estimates of total load depend on how well unsampled flows are represented by sampled flows, estimation of the total number of frames (population total) required to uniquely capture wood load and the estimation of average volume per log. To help refine the methods presented in this paper, future work should focus on analyzing the impacts of data gaps, comparing video monitoring to time-lapse photography in order constrain estimates of population totals and comparing log size measurements from imagery to jams downstream. These wood load estimates are minimum estimates for the time period because they do not include sunken logs or rootwad volumes. Rootwad volumes were not calculated owing to difficulties in estimating volumes and because only a small fraction (7%) of LW monitored had rootwads. Future work that focused on developing relationships to easily estimate drift rootwad volumes would be valuable for estimating total volumes and carbon mass for in- stream LW.

Precision decreased as sampling interval length increased due to smaller sample sizes (Table IV). For example, the percentage error for total wood count increased from 9% for 1 min data to 37% for 15 min data. Thus determining an interval at which to sample becomes a balance between precision desired and equipment, access and post-processing time constraints. Precision can be increased by computing estimates using stratification schemes such as stratifying by day or discharge (Table I). Total count estimates are more precise than total volume estimates (Table IV) due to large uncertainties in the average volume per log. The most gain in precision will be achieved by future work that focuses on reducing the variance in average volume per log. This can be done by experimenting with sampling strategies and increasing the sample size.

It is important to reiterate that the total loads presented here are not estimates of the total seasonal load for the Slave River in 2012 because only the second half of the summer was monitored. Actual wood loads are likely more than twice these values since the larger first freshet peak of the season was not monitored. In 2012 there was no ice jam flood. In years with ice jam flooding, wood transport is likely much higher due to the bulldozing effect of ice and sudden failure of ice jams that release waves of water downstream. Multi-year analysis needs to be conducted to determine if these values are typical for any given year.

Conclusion

This study is part of a larger investigation of wood transport dynamics in large rivers and export of large wood to the Arctic from the Mackenzie Basin, Canada. Prior to the installation of the network of cameras, this study was initiated todetermine the longest sampling interval that achieved unbiased equal variance results and to develop methods to compute wood fluxes and loads from the data. Specifically, this study developed methods to: (i) construct fluvial wood flux curves; (ii) analyze the effects of sample interval lengths on transport estimates (both flux and load); and (iii) estimate total wood loads within a specified time period from coarse-interval ($\geq$1 min) time-lapse photography.

There are many strengths to using time-lapse photography to monitor wood fluxes and loads. It is a low-cost, low-maintenance, power-efficient method. It can be used to extrapolate into data gaps, such as night-time. It produces conservative, first-orderestimates of minimum wood loads. Also, it allows easy comparisons of wood flux to hydrographs on long spatial and broad temporal scales. However, there are several limitations. Estimates are imprecise. Total wood load estimates rely on making several assumptions about representative sampling, log travel times and average log size. Also, sampling is limited to large pieces and has a limited range (approximately $<$60 m for logs $>$10 cm in width and 1 m in length; and $<$300 m for logs greater than $>$20 cm in width and

3 m in length). As mentioned in the Discussion, future work should focus on improving precision, analyzing the effects of data gaps, estimating rootwad volumes, estimating sunken log transport, comparing time-lapse to video monitoring, and identifying intervals that produce unbiased estimates for a variety of drainage sizes, hydrograph regimes and recruitment processes.

Acknowledgements—This project was primarily funded by the Edward M. Warner Graduate Grant awarded by the CSU Geoscience Department, with an additional donation from Charles Blyth. Special thanks to Robin Reich for his knowledge and support and to Water Survey Canada, The Yellow House and the Smith's Landing Band of Fort Smith for data, logistics, and field support. Edward Schenk and one anonymous reviewer greatly improved this manuscript and we are deeply grateful for their constructive and well-thought-out reviews. National Geographic Research Grant 9183-12 funded the acquisition and deployment of a network of cameras in 2013.

References

Abbe TB, Montgomery DR. 2003. Patterns and processes of wood debris accumulation in the Queets river basin, Washington. *Geomorphology* **51**: 81–107.

Battin TJ, Kaplan LA, Findlay S, Hopkinson CS, Marti E, Packman AI, Newbold JD, Sabater F. 2008. Biophysical controls on organic carbon fluxes in fluvial networks. *Nature Geoscience* **1**: 95–100.

Beechie TJ, Sear DA, Olden JD, Pess GR, Buffington JM, Moir H, Roni P, Pollock MM. 2010. Process-based principles for restoring river ecosystems. *BioScience* **60**: 209–222.

Beltaos S, Prowse TD, Carter T. 2006. Ice regime of the lower Peace River and ice-jam flooding of the Peace–Athabasca Delta. *Hydrological Processes* **20**: 4009–4029.

Benda LE, Sias JC. 2003. A quantitative framework for evaluating the mass balance of in-stream organic debris. *Forest Ecology and Management* **172**: 1–16.

Collins BD, Montgomery DR, Fetherston KL, Abbe TB. 2012. The floodplain large-wood cycle hypothesis: a mechanism for the physical and biotic structuring of temperate forested alluvial valleys in the North Pacific coastal ecoregion. *Geomorphology* **139**: 460–470.

Corenblit D, Baas ACW, Bornette G, Darrozes J, Delmotte S, Francis RA, Gurnell AM, Julien F, Naiman RJ, Steiger J. 2011. Feedbacks between geomorphology and biota controlling earth surface processes and landforms: a review of foundation concepts and current understandings. *Earth-Science Reviews* **106**: 307–331.

Everett RA, Ruiz GM. 1993. Coarse woody debris as a refuge from predation in aquatic communities. *Oecologia* **93**: 475–486.

Gibson JJ, Prowse TD, Peters DL. 2006. Hydroclimatic controls on water balance and water level variability in Great Slave Lake. *Hydrological Processes* **20**: 4155–4172.

Gonor JJ, Sedell JR, Benner PA. 1988. What we know about large trees in estuaries, in the sea, and on coastal beaches. In *From the Forest to the Sea: A Story of Fallen Trees*, Maser C, Tarrant RF, Trappe JM, Franklin JF (eds). USDA Forest Service General Technical Report GTR-PNW-229. Pacific Northwest Research Station: Portland, OR; 83–112.

Gurnell A, Tockner K, Edwards P, Petts G. 2005. Effects of deposited wood on biocomplexity of river corridors. *Frontiers in Ecology and the Environment* **3**: 377–382.

Heathfield DK, Walker IJ. 2011. Analysis of coastal dune dynamics, shoreline position, and large woody debris at Wickaninnish Bay, Pacific Rim National Park, British Columbia. *Canadian Journal of Earth Sciences* **48**: 1185–1198.

Jones CE, Hinzman LD, Kielland K. 2013. Integrating Alaskan local knowledge and science to model driftwood harvest from the Yukon River in a changing climate. In *AWRA Annual Water Resources Conference*, Portland, OR, November 2013.

Lamlom S, Savidge R. 2003. A reassessment of carbon content in wood: variation within and between 41 North American species. *Biomass and Bioenergy* **25**(4): 381–388. DOI:10.1016/S0961-9534(03)00033-3

MacVicar B, Piégay H. 2012. Implementation and validation of video monitoring for wood budgeting in a wandering piedmont river, the Ain River (France). *Earth Surface Processes and Landforms* **37**: 1272–1289.

Moulin B, Schenk ER, Hupp CR. 2011. Distribution and characterization of in-channel large wood in relation to geomorphic patterns on a low-gradient river. *Earth Surface Processes and Landforms* **36**: 1137–1151.

Naiman RJ, Balian EV, Bartz KK, Bilby RE, Latterell JJ. 2002. Dead wood dynamics in stream ecosystems. In *Proceedings of the Symposium on the Ecology and Management of Dead Wood in Western Forests*; 23–48.

Polvi L, Wohl E. 2013. Biotic drivers of stream planform: implications for understanding the past and restoring the future. *BioScience* **63**: 439–452.

Ruiz Villanueva V, Castellet EB, Díez-Herrero A, Bodoque JM, Sánchez-Juny M. 2013. Two dimensional modelling of large wood transport during flash floods. *Earth Surface Processes and Landforms* doi: 10.1002/esp.3456.

Scheaffer RL, Mendenhall W III, Ott LR, Gerow KG. 2012. *Survey Sampling* (7th intl edn). Brooks/Cole – Cengage Learning: Stamford, CT.

Schenk ER, Moulin B, Hupp CR, Richter JM. 2013. Large wood budget and transport dynamics on a large river using radio telemetry. *Earth Surface Processes and Landforms*doi: 10.1002/esp.3463.

Skalak K, Pizzuto J. 2010. The distribution and residence time of suspended sediment stored within the channel margins of a gravel- bed bedrock river. *Earth Surface Processes and Landforms* **35**: 435–446.

West AJ, Lin C-W, Lin T-C, Hilton RG, Liu S-H, Chang C-T, Lin, K-C, Galy A, Sparkes RB, Hovius N. 2011. Mobilization and transport of coarse woody debris to the oceans triggered by an extreme tropical storm. *Limnology and Oceanography* **56**: 77–85.

Wohl E, Dwire K, Sutfin N, Polvi L, Bazan R. 2012. Mechanisms of carbon storage in mountainous headwater rivers. *Nature communications* **3**: 1263.

